J. Fluid Mech. (1997), *vol.* 351, *pp.* 345–357. Printed in the United Kingdom

Stabilization of a cylindrical capillary bridge far beyond the Rayleigh–Plateau limit using acoustic radiation pressure and active feedback

By MARK J. MARR-LYON, DAVID B. THIESSEN AND PHILIP L. MARSTON

Department of Physics, Washington State University, Pullman, WA 99164-2814, USA

(Received 7 February 1997 and in revised form 1 June 1997)

A novel method of suppressing the Rayleigh–Plateau capillary instability of a cylindrical liquid bridge is demonstrated which uses the radiation pressure of an ultrasonic wave to control the shape of the bridge. The shape of the bridge is optically sensed and the information used to control the spatial distribution of the radiation stress on the surface of the bridge. The feedback is phased so as to suppress the growth of the axisymmetric mode which normally becomes unstable when the slenderness, given by the length to diameter ratio, exceeds π. Stabilization is achieved out to a slenderness of 4.3 for a bridge density matched to the surrounding water bath in a Plateau tank. Breakup of such long bridges was found to produce a satellite drop from the receding thread of liquid. The active stabilization mechanism used may have application to other capillary systems.

1. Introduction

Plateau (1863) studied the surface-tension-driven instability of cylindrical liquid surfaces and the problem was analysed by Rayleigh (1879). In the absence of gravity, a cylindrical liquid column of length L and radius R with pinned contact lines becomes unstable and breaks if the slenderness $S = L/2R$ exceeds π. This length is usually known as the Rayleigh–Plateau (RP) limit. The control of the RP instability is relevant to the management of fluids in various situations. For example, fluid handling schemes in the reduced-gravity environment of an orbiting spacecraft can make use of cylindrical liquid columns. In some instances it may be advantageous to have an extra-long liquid column, such as in a float-zone crystal growth operation. Stabilization methods relying on specific electrical properties of the liquid column have been studied. Bridge stabilization at lengths beyond the RP limit has been demonstrated using axial electric fields for dielectric fluids (Raco 1968; Sankaran & Saville 1993; Ramos, Gonzalez & Castellanos 1994). An axial magnetic field has been predicted to stabilize bridges of conducting liquids (Nicolás 1992). The stabilization method demonstrated here uses a fundamentally different approach.

A bridge stabilization method will be described in this paper which uses acoustic radiation pressure – the time-averaged pressure of an acoustic standing wave – to preferentially expand one side or the other of a liquid bridge, counteracting the growth of the mode of deformation which normally leads to breakup of the bridge. The radiation pressure of an acoustic standing wave is commonly used to trap and manipulate drops or bubbles in low-gravity environments (Marston *et al.* 1994;

Wang, Anilkumar & Lee 1996; Apfel *et al.* 1997). It provides a convenient way of driving shape oscillations on drops or bubbles by modulation of the acoustic radiation pressure (Marston & Apfel 1979; Marston 1980; Trinh, Zwern & Wang 1982; Trinh, Marston & Robey 1988; Asaki & Marston 1995*a*). Morse, Thiessen & Marston (1996) have shown that modulation of acoustic radiation pressure can be used to excite various shape modes of a cylindrical liquid bridge in a Plateau tank.

The method of stabilization described here appears to offer a unique way of observing the breakup of a long low-viscosity axisymmetric fluid column. Breakup in this experiment can follow a quiescent initial condition with a cylindrical geometry at a slenderness ratio which is well into the naturally unstable region. It can be initiated by turning off the ultrasonic field that stabilizes the bridge. Photographic evidence to be presented here reveals the existence of a thin axisymmetric neck during the final stages of breakup. Such necks are characteristic of the pinch-off of a hanging droplet or a liquid jet which has received much attention in the literature. The dynamics of breakup are interesting because they involve a singularity in the continuum equations as the neck diameter approaches zero. Universal scaling laws have been shown to apply in the vicinity of the singularity which lead to similarity solutions for the shape of the neck (Eggers 1993). Studies of pinch-off for a drop falling from a nozzle (Shi, Brenner & Nagel 1994) and of the breakup of drops which have been stretched in a Couette flow (Tjahjadi, Stone & Ottino 1992) confirm some aspects of the theory. Other experiments relevant to breakup include those on stretching of liquid bridges by Zhang, Padgett & Basaran (1996).

The Bond number of a capillary bridge is commonly defined as

$$B = (\rho_i - \rho_o)\,\frac{gR^2}{\sigma},$$

where ρ_i and ρ_o are the densities of the inner and outer fluids, g is the acceleration due to gravity, and σ is the interfacial tension. For the experiments described here, B is quite small ($|B| \approx 10^{-3}$) and the small offset in B from zero which may be present is unimportant to the interpretation of the observations. The experimental configuration chosen for convenience has a horizontal bridge axis, though the orientation of the bridge axis relative to the direction of g should be unimportant to the acoustic stabilization mechanism investigated provided $|B|$ is small. A different hydrodynamic stabilization mechanism has recently been investigated by Lowry & Steen (1995, 1997) which is relevant to vertical bridges typically with $|B| \approx 0.01$ and values of S much closer to the RP limit than is the emphasis of the present paper.

The oscillation modes of a capillary bridge are associated with surface deformations which can be characterized in terms of an axial index N and azimuthal index m. The index N is the number of half-wavelengths in the axial direction, while m is the number of wavelengths in the azimuthal direction (Sanz & Díez 1989). The axial surface deformations are not purely sinusoidal owing to the conditions of volume conservation and zero fluid velocity at the end supports. Axisymmetric modes have $m = 0$, and in the absence of stabilization the $(N, m) = (2, 0)$ capillary mode is the first mode predicted to become unstable as S is increased with $B = 0$. Only the growth of the $(2, 0)$ mode is suppressed in this experiment. Normalized mode frequencies for the $(2, 0)$ and $(3, 0)$ axisymmetric and the $(1, 1)$ and $(1, 2)$ non-axisymmetric modes for the system of liquids used here were measured by Morse *et al.* (1996) for $S < 3.1$. Some other investigations of the dynamics of bridges with small B include Zhang & Alexander (1990) and Perales & Meseguer (1992) while Anilkumar *et al.* (1993), in an experiment carried out at moderately large B, demonstrated that vibration of one

end of a bridge introduces a streaming that may be used to balance thermocapillary flow.

2. Relevant aspects of acoustic radiation pressure

Prior to considering the mechanism of acoustic stabilization it is helpful to review some properties of the acoustic radiation pressure on liquid drops in ultrasonic standing waves. Attention is restricted to the case which is analogous to the liquid bridge used in our experiment where $\rho_i \approx \rho_o$ and the ratio of the inner to outer adiabatic compressibilities κ_i/κ_o is greater than unity. Furthermore, as in our experiment, the radius R is small in comparison to the acoustic wavelength but large in comparison to the thickness of the Stokes boundary layers which oscillate at the acoustic frequency. For this situation, the viscous corrections to the radiation force have been shown to be small (Doinikov 1994, 1997) so that the inviscid acoustic approximation of Yosioka & Kawasima (1955) is applicable. Observations for this situation (Crum 1971; Apfel 1976; Marston & Apfel 1979; Trinh *et al.* 1982) confirm the predictions that the radiation force on the drop is directed toward the pressure antinodes of the standing wave.

The equilibrium shape is predicted to be non-spherical so as to establish a balance between the local radiation stresses and the Young–Laplace pressure (Marston 1980; Jackson, Barmatz & Shipley 1988). The radiation stress analysis of Asaki & Marston (1995*b*), given originally for bubbles, may be shown to apply to this case with the following prediction: the small drop under consideration with $\rho_i \approx \rho_o$ and $\kappa_i > \kappa_o$ located at a pressure antinode will be flattened with its symmetry axis along the opposing wavevectors of the acoustic standing wave. The deformation varies in proportion to p_a^2/σ when p_a is small where p_a is the acoustic pressure amplitude.

Both from the direction of the radiation force and from the predicted flattening of the drop, it is evident that parcels of the more compressible fluid in the density-matched system are attracted to the pressure antinode of the standing wave. An energy analysis also supports this conclusion (Gor'kov 1962). The design of the experiment described below may be anticipated from a generalization of this result to capillary bridges.

3. Experimental apparatus

3.1. *The Plateau tank and the acoustic control strategy*

A liquid bridge is deployed between two circular supports of radius $R = 2.16$ mm in water in a transparent acrylic Plateau tank (figure 1). The bridge liquid is a mixture of 5 cS polydimethylsiloxane (PDMS, Dow Corning 200 fluid, density $\rho_{PDMS} = 0.92\ \mathrm{g\,cm^{-3}}$, compressibility $\kappa_{PDMS} = 11.9\times10^{-11}\ \mathrm{cm^2\,dyne^{-1}}$) and tetrabromoethane (TBE, density $\rho_{TBE} = 2.96\ \mathrm{g\,cm^{-3}}$, compressibility $\kappa_{TBE} = 3.11\times10^{-11}\ \mathrm{cm^2\,dyne^{-1}}$). A composition of 11.3% by weight TBE in PDMS gives the bridge liquid the same density as water so the bridge is neutrally buoyant within a small experimental error. The interfacial tension between this mixture and water was measured to be 36 dyne $\mathrm{cm^{-1}}$ at 21 °C using a static method based on digital image analysis. A simple mixing rule was used to determine the compressibility of the PDMS and TBE mixture, which gives a compressibility ratio of $\kappa_i/\kappa_o = 2.6$.

A 5.1 cm diameter resonant-bar transducer driven by a stack of piezoelectric disks is mounted in the base of the Plateau tank. The transducer is modified from the one

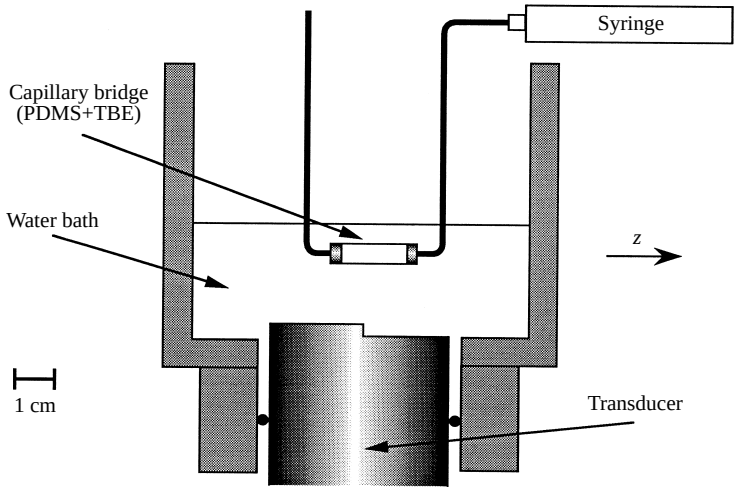

FIGURE 1. Front view of the Plateau tank with a stepped transducer.

described by Morse *et al.* (1996) in that the transducer has a 3 mm step machined into the radiating surface along a diameter (figure 1). The transducer is driven at approximately 120 kHz with a water height of 3.1 cm above the low side of the transducer. This produces an acoustic standing wave inside the tank having spatial structure that depends on the frequency because the distance to the reflecting surface opposite the transducer has a left–right (l–r) asymmetry when viewed as in figure 1. Scanning the tank with a small hydrophone revealed the presence of a pressure antinode that moved horizontally in space as a function of driving frequency. (The frequency dependence of the location of the antinode in an acoustic resonator having a step in the boundary was also confirmed with an approximate numerical solution of the wave equation.) The property of acoustic radiation pressure reviewed in §2 that the most compressible fluid is attracted to the pressure antinode is used to control the shape of the bridge. The bridge is positioned in the sound field such that the antinode is roughly in the centre of the bridge and can be moved slightly off centre in either direction. Thus, by adjusting the frequency the acoustic radiation pressure can be positioned to expand either half of the bridge. Notice that since the vertical position of the bridge is close to an antinode, the up–down radiation pressure forces on the bridge are weak. Consequently, varying the acoustic frequency primarily couples to the $(2,0)$ capillary mode and only weakly to the $(1,1)$ and $(2,1)$ translational modes of the bridge. Typically, the acoustic pressure amplitude at the antinode was approximately 1.4 atm.

3.2. *Optical sensor*

The purpose of the optical sensor is to detect the l–r asymmetry of the $(2,0)$ capillary mode. A schematic of the optics is shown in figure 2(a). The bridge is illuminated with a HeNe laser beam that has been expanded to about 15 mm in diameter. After passing through the bridge, the beam is focused onto a 10 mm diameter four-segment photodiode. A spatial filter placed at the focus of the lens blocks light reflected and refracted by the bridge from entering the photodiode. The detected optical power is reduced in proportion to the extinction of light by the bridge though it does not give a true measurement of the optical extinction as noted in some of the previous applications of this detection method (Trinh *et al.* 1988; Stroud & Marston 1993).

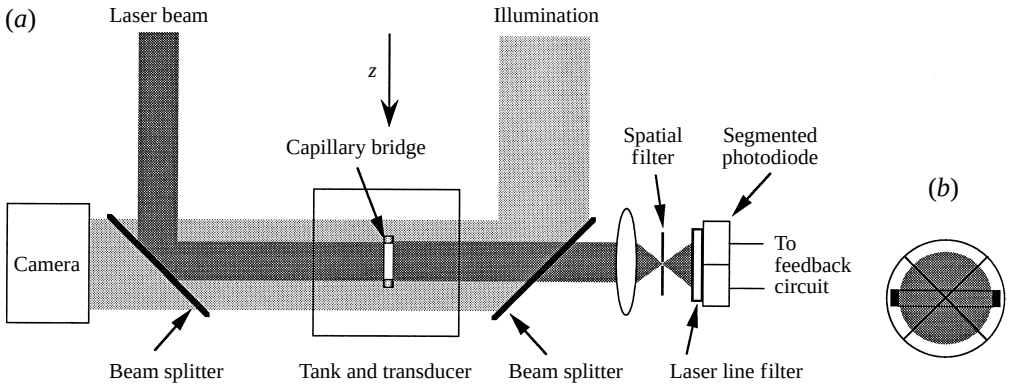

FIGURE 2. Top view of optical arrangement (*a*), and photodiode orientation (*b*). The grey circle represents the spot size of the laser beam illuminating the photodiode.

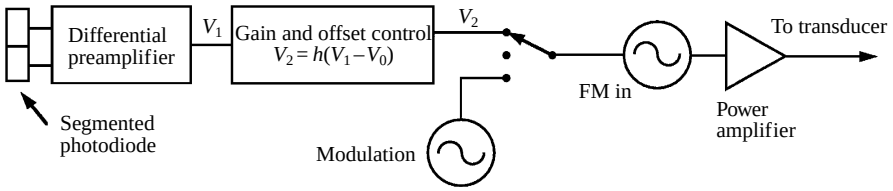

FIGURE 3. Electronics block diagram.

The aperture of the spatial filter is sufficiently wide to avoid modulation of the detected optical power by the acoustic standing wave. It is also wide enough to pass the forward diffraction peak of the bridge. A laser line filter is also used to reduce noise caused by room lighting. The use of beam splitters allows the bridge to be backlit and viewed with either a CCD or 35 mm SLR camera. The photodiode is oriented with respect to the projected bridge image as shown in figure 2(*b*). In this orientation, only two of the four segments are used. The photodiode is mounted on a translation stage to allow fine adjustment in the horizontal direction perpendicular to the laser beam.

3.3. *Feedback and electronics*

The photodiode signals are input to the circuit illustrated in figure 3. In the preamplifier, the currents produced by the photodiode are converted into voltages and the difference, V_1, is taken. Then an adjustable offset voltage V_0 is subtracted from V_1 and the difference is multiplied by an adjustable gain h. For active control V_2 is applied to the frequency modulation input of a function generator which produces a sine wave of frequency $f = f_0(1 + KV_2)$. The centre frequency f_0 is typically about 120 kHz, and during normal stabilization f will vary by less than 1 kHz. The output of the generator is amplified and applied to the transducer. The feedback signal V_2 may be disconnected with the switch shown in figure 3, and for test purposes it can be helpful (see §4) to replace V_2 by a low-frequency sine wave so as to purposely excite the $(2, 0)$ mode of a naturally stable bridge.

The asymmetric acoustic radiation pressure profile applied to the bridge can be seen as an equivalent force applied to a damped mass-and-spring system. A linear model for a capillary bridge with feedback is discussed in the Appendix. Increasing the gain of the feedback system has the effect of stiffening the spring. A bridge which is longer

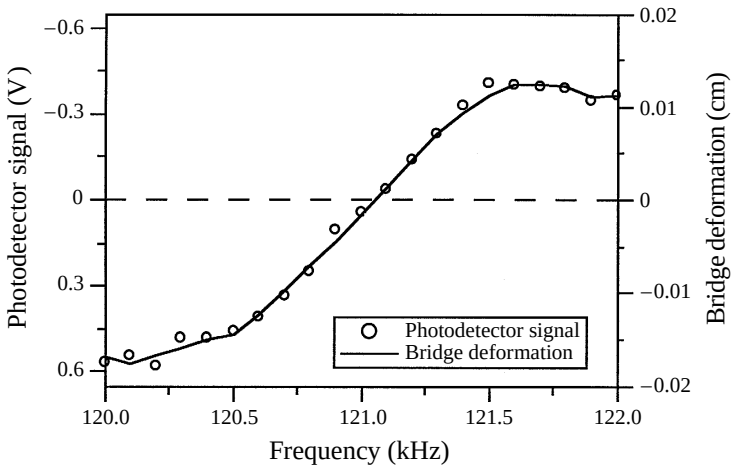

FIGURE 4. Static bridge deformation and photodetector signal as a function of driving frequency for a bridge of $S = 3.0$.

than the RP limit would have a negative spring constant, leading to instability. The effect of feedback is to make the effective spring constant positive thus stabilizing the system.

4. Control of the equilibrium shape of a naturally stable bridge

The stabilization scheme utilized in this work depends on the idea that the asymmetric sound field in the tank produces a radiation pressure difference between the halves of the bridge, and that this difference is linearly related to the transducer driving frequency. The design of the feedback control system is also based on the assumption that the photodetector signal is linearly related to the actual bridge deformation. To test these assumptions a bridge with slenderness slightly less than the RP limit was deployed in the sound field and the acoustic frequency was slowly varied. Figure 4 is a plot of the bridge deformation as a function of acoustic frequency measured by digital image analysis superimposed with the photodetector signal from the light extinction system. The deformation is measured by locating the coordinates of several hundred edge points for the top and bottom edges of the horizontal bridge from a digital image. The bridge radius $R_{meas}(z)$ at a given axial point z is taken as one-half the diameter measured at that point. The bridge radius can be expanded in a Fourier series

$$R(z) = R_0 + c_1 \sin\left(\frac{\pi z}{L}\right) + c_2 \sin\left(\frac{2\pi z}{L}\right) + \ldots,$$

where the Fourier coefficient c_2 is termed the 'bridge deformation' in figure 4. To find c_2, the integral

$$c_2 = \frac{2}{L}\int_0^L R_{meas}(z) \sin\left(\frac{2\pi z}{L}\right) \mathrm{d}z$$

is evaluated numerically. The photodetector signal plotted is the difference between the signal measured at point V_1 in figure 3 and the signal measured for a bridge with zero deformation. It is clear that over a range of frequencies, the bridge deformation is approximately a linear function of frequency, and the photodetector signal is in

good agreement with the actual bridge shape. This is the region in which stabilization can take place.

An additional test of the coupling is to replace V_2 by a low-frequency sine wave so as to modulate the acoustic frequency. When the frequency of the modulation is adjusted to the natural frequency of the $(2,0)$ mode, the bridge is observed to be driven into stable oscillation in that mode. The mode frequency was found to decrease with increasing slenderness $S < \pi$ as previously confirmed by Morse *et al.* (1996) using only amplitude modulation of the ultrasonic standing wave.

5. Bridge stabilization

5.1. *Experimental procedure*

A naturally stable cylindrical bridge with $S \approx 3$ is produced in the absence of a sound field. The position of the photodiode is adjusted such that the output voltage, V_1 in figure 3, is nearly zero. At this point, a sound field is applied without feedback and the centre frequency is adjusted such that V_1 is again nearly zero. Feedback is now turned on, and the bridge shape is fine tuned by adjusting V_0. The bridge is extended by separating the supports while injecting fluid to maintain a cylindrical volume. The gain h must be adjusted such that it is high enough to enable the bridge to be extended past the RP limit. However, it has been observed that if the gain is set too high, the bridge will be driven into oscillation. One possible explanation for this is that the time delay between the measurement of the bridge shape and the application of the restoring force causes a reduction in the effective damping. At large enough feedback gain the damping will become negative, causing the bridge to become unstable (see the Appendix), although it is unknown if this is the mechanism that causes the observed instabilities.

5.2. *Results*

Figure 5 shows a sequence of images captured from a CCD video record of a stabilized bridge. In figure 5(*a*), there is no sound field and the bridge is naturally stable at $S = 3.0$. The stabilization is then turned on and the bridge extended to $S = 4.1$ (figure 5*b*). The bridge remains stable for approximately 4.5 minutes (figure 5*b–d*). At the time shown in figure 5(*d*), the sound field is turned off and within about 0.5 s the bridge is broken (figure 5*e–h*). The time code displayed in the upper left corner of each image is in the format 'hours:minutes:seconds:frames:field', where there are 30 frames per second and 2 fields per frame. Each field was exposed for $1/10\,000$ s.

The amount of time a bridge will remain stable when extended past the RP limit decreases the longer the bridge. Since the bridge is not completely isolated from the environment, small low-frequency ambient vibrations appear to eventually cause the bridge to become unstable so that it breaks. Bridges with $S \approx 3.8$ have remained stable for up to 45 minutes, while bridges with $S \approx 4.3$ are stable for up to several minutes. Figure 6 is a photograph of a stabilized bridge having $S = 4.3$. The static l–r asymmetry evident is more pronounced than for the slightly shorter bridge in figure 5(*c*). A small amount of rotational asymmetry is also evident and these imperfections are to be expected from the static responses to the radiation stress noted in §2. The imperfections are more clearly seen the more slender the bridge. The small amplitude of these asymmetries may be a consequence of the relatively large variation of radiation pressure with location on the surface of the bridge needed to excite modes having $m > 1$ in comparison to the $(2,0)$ mode. For the present case of a bridge located at a pressure antinode, this variation is small because the ratio

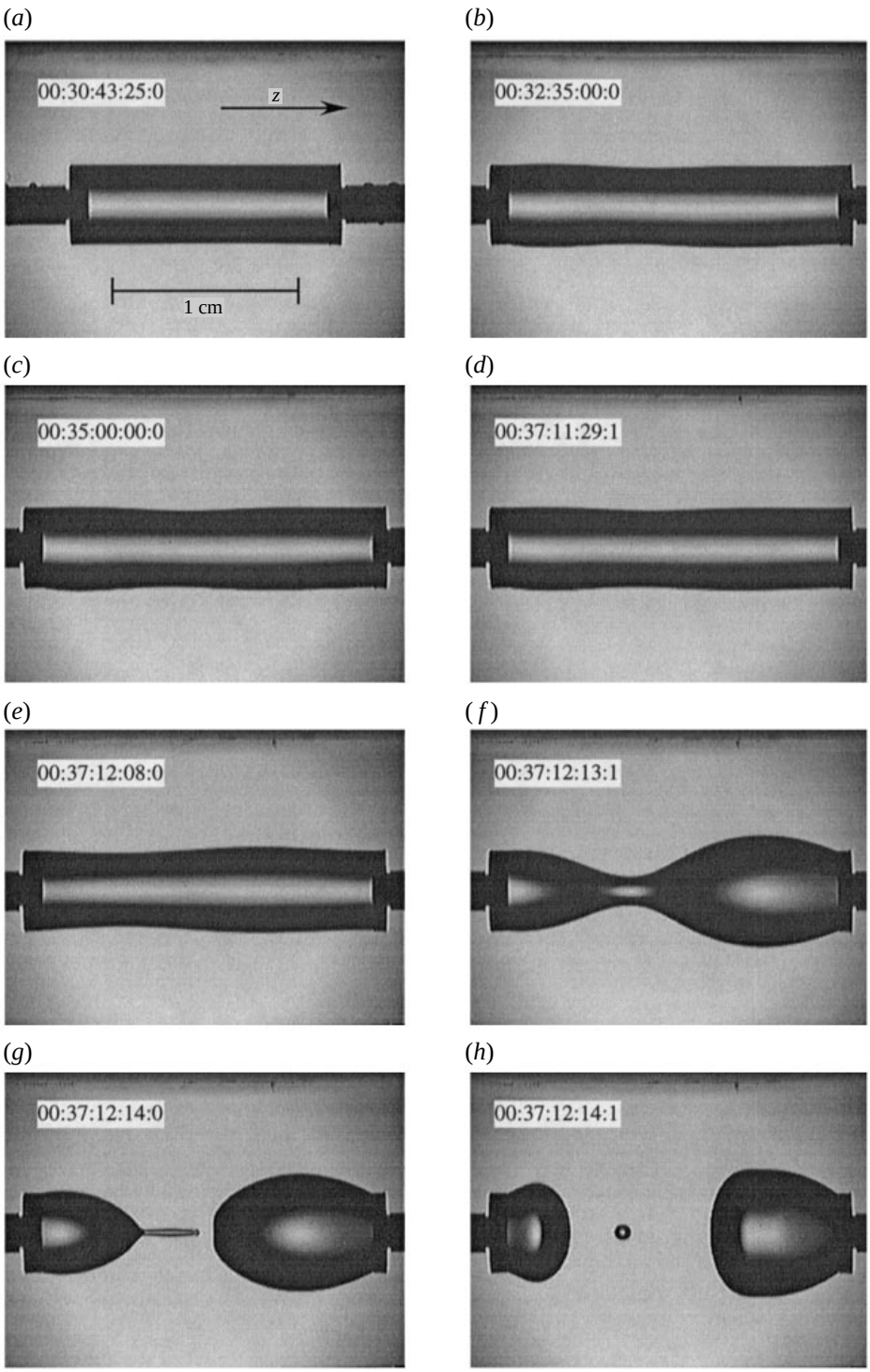

FIGURE 5. A CCD record of a stabilized bridge. In (*d*) the sound is turned off resulting in growth of the (2, 0) mode and subsequent breakup of the bridge.

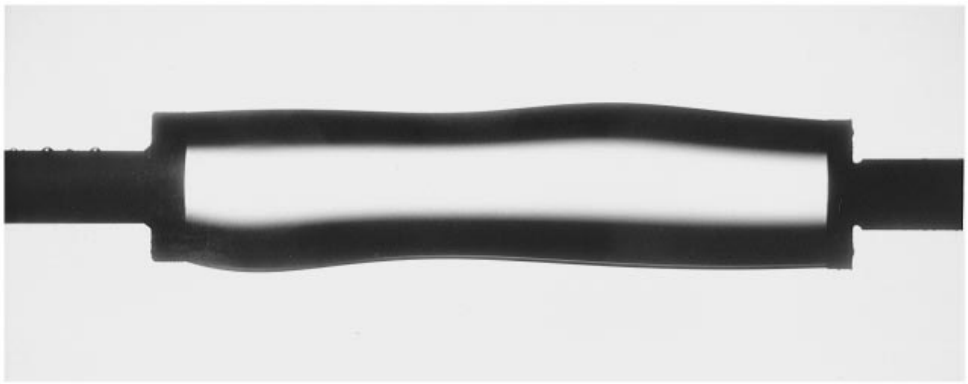

FIGURE 6. A stabilized bridge with $S = 4.3$.

of R_0 to the acoustic wavelength is only 0.18. It is also relevant that a given modal amplitude for $m > 1$ is associated with relatively large variations in the mean surface curvature and hence large variations in pressure. Deformations having $m = 1$ have been suppressed because the variations in the translational force with axial position are suppressed by the positioning of the bridge at an antinode as discussed in §3.1.

The intentional breakup of a long bridge may be triggered as in figure 5(*d*) by switching off the input to the power amplifier that drives the acoustic transducer. The resulting breakup always generates a satellite drop as shown in figure 5(*h*). Notice also in figure 5(*g*) that the left surface of the drop attached to the rightmost support appears to be flattened by the momentum of the receding column of liquid. For the range of bridge lengths explored the initiation of the breaking of the bridge appears to be associated with the growth of the (2, 0) mode as is evident by inspection of figure 5(*c*).

6. Discussion and conclusions

It has been demonstrated that acoustic radiation pressure can be used with an active feedback system to stabilize capillary bridges in simulated low gravity well beyond the RP limit. With the current apparatus, stable bridges with S as large as 4.3 can be produced.

In the event that perfect control of the (2, 0) mode were achieved by the active feedback method demonstrated, it is anticipated that for a sufficiently long bridge, the (3, 0) mode becomes unstable. A simple generalization of Rayleigh's analysis indicates that the stability limit for the (3, 0) mode is $S = 3\pi/2 \approx 4.71$. While it is not known if our method may be used to reach that limit, it is noteworthy that for more viscous liquids than the approximately 5 cS mixture used here, it should be possible to increase the amplification of the feedback loop without driving the bridge into oscillations. The linear inviscid analysis of Sanz (1985) and Sanz & Díez (1989) predicts that the (3, 0) mode frequency vanishes for $S = 3\pi/2$ while the non-axisymmetric mode frequencies remain finite. To suppress the growth of the (3, 0) mode in a sufficiently slender bridge by active feedback, it would be necessary to add an additional degree of freedom to the sensor and to the control of the radiation pressure distribution. This would probably require a significant complication of the ultrasonic transducer.

While the positioning of the bridge in the acoustic field was selected for the present case of a neutrally buoyant bridge, the radiation-pressure feedback control

demonstrated here may be applied to stabilize liquid bridges surrounded by gas. Unfortunately, the stability limits of a cylindrical bridge in that case might be best explored in a reduced gravity environment.

This work was supported by NASA.

Appendix. Linear model for the effect of feedback on bridge stability

A linear model of a capillary bridge in an external bath was explored to study the effect of feedback on bridge stability. The model includes through a choice of parameters the effects of an external bath and of an applied radiation pressure on the bridge which counteracts the growth of the $(2,0)$ mode. The important result obtained below is that for a naturally unstable bridge there is a limited range of feedback strengths for which the bridge is expected to be stabilized. The bridge response is analogous to that of a driven, damped, harmonic oscillator, where the $(2,0)$ mode amplitude x corresponds to the oscillator's displacement. Since a liquid surface has a characteristic energy per unit area (surface tension), the change in potential energy associated with a deformed neutrally buoyant bridge arises from a change in surface area. It follows from geometric considerations that for the $(2,0)$ mode the change in surface area and thus in potential energy is proportional to $[(\pi/S)^2 - 1]x^2$ (Rayleigh 1879). Since the potential energy of a harmonic oscillator with spring constant k is $kx^2/2$, the spring constant for the $(2,0)$ mode is seen to be proportional to $[(\pi/S)^2 - 1]$. The generalized force on the modal mass is the sum of the spring, damping, and feedback generalized forces. The feedback force is taken to be a constant times the position of the mass at some previous time which approximates the time required to sample the mode displacement. The total force is

$$F_{tot}(t) = -kx(t) - \gamma \frac{\mathrm{d}x}{\mathrm{d}t} - Gx(t-\tau) - \alpha\sqrt{2}\int_{-\infty}^{t} \frac{1}{[\pi(t-t')]^{1/2}} \frac{\mathrm{d}^2x}{\mathrm{d}t'^2}\mathrm{d}t', \qquad (A\,1)$$

where k is the spring constant, γ is the usual damping coefficient, G is the feedback gain, τ is the time lag between the position measurement and the application of the feedback force, and α is a boundary-layer coefficient. The boundary-layer term, which includes both the viscous damping and inertia of the boundary layer, is of the form given by Dryden, Murnaghan & Bateman (1956) and for shape oscillations of drops by Prosperetti (1977). Expressions for the real, positive coefficients γ and α are not given here but they could be approximated by extending the analysis of Higuera, Nicolás & Vega (1994) to include the viscosity and inertia of the outer bath. The equation of motion for the modal amplitude becomes

$$F_{tot} = m_b \frac{\mathrm{d}^2x}{\mathrm{d}t^2}, \qquad (A\,2)$$

where m_b denotes the 'bare' modal effective mass for the corresponding inviscid system (Sanz 1985). Solutions of the form

$$x = x_0\,\mathrm{e}^{\mathrm{i}\Omega t} \qquad (A\,3)$$

were investigated where Ω is a complex frequency and the integral in (A 1) is a half-order derivative of $\mathrm{d}x/\mathrm{d}t$ (Oldham & Spanier 1974). The feedback force becomes

$$F_{feedback} = -Gx_0\,\mathrm{e}^{-\mathrm{i}\Omega\tau}\,\mathrm{e}^{\mathrm{i}\Omega t}. \qquad (A\,4)$$

For small values of τ we can approximate $e^{-i\Omega\tau}$ by a Taylor series expansion about $\tau = 0$ through terms second order in τ. Substituting for x from (A 3) in (A 2) yields the following characteristic equation for Ω:

$$(\omega_b^2 + G_e) - (1 + \tfrac{1}{2}G_e\tau^2)\Omega^2 + \alpha_e i(1+i)\Omega^{3/2} + i(\gamma_e - G_e\tau)\Omega = 0,$$

where $\omega_b^2 = k/m_b$ and ω_b is the natural frequency of the 'bare' or inviscid system (Sanz 1985), $G_e = G/m_b$, $\alpha_e = \alpha/m_b$, and $\gamma_e = \gamma/m_b$. The characteristic equation can be cast in the more convenient form for comparing to previous results

$$\omega_n^2 - \Omega^2 + \alpha_n i(1+i)\Omega^{3/2} + i\gamma_n\Omega = 0, \tag{A 5}$$

in which the following normalized quantities appear:

$$\omega_n^2 = \frac{\omega_b^2 + G_e}{1 + \frac{1}{2}G_e\tau^2}, \quad \alpha_n = \frac{\alpha_e}{1 + \frac{1}{2}G_e\tau^2}, \quad \gamma_n = \frac{\gamma_e - G_e\tau}{1 + \frac{1}{2}G_e\tau^2}. \tag{A 6a–c}$$

Because of the feedback loop, ω_n^2 may be made to be real and positive even though the natural spring constant k and ω_b^2 are negative. The discussion below concerns only the cases of interest which have $\omega_n^2 > 0$. Equation (A 5) is now in the same form, apart from some higher-order terms, as (6) of Asaki & Marston (1995) which was derived for oscillating drops or bubbles immersed in a second fluid in a situation where $G_e = 0$. Asaki & Marston (1995) give the following asymptotic solution to the characteristic equation where $\omega_n^2 > 0$:

$$\begin{aligned}\Omega = \omega_n - \frac{\alpha_n\omega_n^{1/2}}{2} + \frac{7\sqrt{2}\alpha_n^3}{32\omega_n^{1/2}} - \frac{3\alpha_n\gamma_n}{8\omega_n^{1/2}} - \frac{5\alpha_n^4}{32\omega_n} + \frac{3\alpha_n\gamma_n}{8\omega_n} - \frac{\gamma_n^2}{8\omega_n} \\ + i\left(\frac{\gamma_n}{2} + \frac{\alpha_n\omega_n^{1/2}}{2} - \frac{\alpha_n^2}{2} + \frac{7\sqrt{2}\alpha_n^3}{32\omega_n^{1/2}} - \frac{3\alpha_n\gamma_n}{8\omega_n^{1/2}}\right) + O(\omega_n^{-3/2}).\end{aligned} \tag{A 7}$$

The stability of the bridge is indicated by the sign of the imaginary part of Ω, a negative sign indicating instability. However, this asymptotic solution in (A 7) is based on the assumptions that $(\alpha_n/2) < \omega_n^{1/2}$ and $(\gamma_n/2) < \omega_n$. According to this model, feedback has the desirable effect of raising the effective spring constant, which raises ω_n^2 according to (A 6 a). Without feedback, the mass-and-spring system becomes unstable if the spring constant is negative. In the bridge model the spring constant for the $(2,0)$ mode is proportional to $(\pi/S)^2 - 1$, where S is the slenderness. It becomes negative when $S > \pi$. The addition of feedback can turn a negative spring constant into a positive effective spring constant thus allowing stabilization of bridges beyond the RP limit. Feedback also influences the normalized damping of the bridge and two competing effects can be seen. The feedback delay causes a reduction in γ_n as the gain is increased. On the other hand an increase in gain increases the resonant frequency which increases the boundary layer damping due to the term $(\alpha_n/2)\omega_n^{1/2}$. The model predicts that as the feedback gain is increased for a given delay τ the damping initially increases but then decreases to the point that the bridge becomes unstable. For a given bridge slenderness in the naturally unstable regime, the model predicts stability for a limited range of feedback gain such that $-\omega_b^2 < G_e < G_{eu}$ where for small α_e, the upper bound G_{eu} becomes γ_e/τ. Experiments (§5) confirm that a bridge with slenderness beyond the RP limit becomes unstable if the feedback gain is reduced or increased too much. According to this model, bridges sufficiently slender that $-\omega_b^2 > \gamma_e/\tau$ may no longer be stabilized; however the assumptions noted below (A 7) may no longer apply. It is appropriate to note that while the feedback

model used in (A 1) is that of a causal distortionless linear-phase filter, the concerns raised by this analysis apply to a broader class of linear-phase low-pass models of the feedback (Papoulis 1962, Chapter 6).

REFERENCES

Anilkumar, A. V., Grugel, R. N., Shen, X. F., Lee, C. P. & Wang, T. G. 1993 Control of thermocapillary convection in a liquid bridge by vibration. *J. Appl. Phys.* **73**, 4165–4170.

Apfel, R. E. 1976 Technique for measuring the adiabatic compressibility, density, and sound speed of submicroliter liquid samples. *J. Acoust. Soc. Am.* **59**, 339–343.

Apfel, R. E., Tian, Y., Jankovsky, J., Shi, T., Chen, X., Holt, R. G., Trinh, E. H., Croonquist, A., Thornton, K. C., Sacco, A., Coleman, C., Leslie, F. W. & Matthiesen, D. H. 1997 Free oscillations and surfactant studies of superdeformed drops in microgravity. *Phys. Rev. Lett.* **78**, 1912–1915.

Asaki, T. J. & Marston, P. L. 1995*a* Free decay of shape oscillations of bubbles acoustically trapped in water and sea water. *J. Fluid Mech.* **300**, 149–167.

Asaki, T. J. & Marston, P. L. 1995*b* Equilibrium shape of an acoustically levitated bubble driven above resonance. *J. Acoust. Soc. Am.* **97**, 2138–2143.

Crum, L. A. 1971 Acoustic force on a liquid droplet in an acoustic stationary wave. *J. Acoust. Soc. Am.* **50**, 157–163.

Doinikov, A. A. 1994 Acoustic radiation pressure on a compressible sphere in a viscous fluid. *J. Fluid Mech.* **267**, 1–21.

Doinikov, A. A. 1997 Acoustic radiation pressure on a spherical particle in a viscous heat-conducting fluid. III. Force on a liquid drop. *J. Acoust. Soc. Am.* **101**, 731–740.

Dryden, H. L., Murnaghan, F. P. & Bateman, H. 1956 *Hydrodynamics.* Dover.

Eggers, J. 1993 Universal pinching of 3D axisymmetric free-surface flow. *Phys. Rev. Lett.* **71**, 3458–3460.

Gor'kov, L. P. 1962 On the forces acting on a small particle in an acoustical field in an ideal fluid. *Sov. Phys. Dokl.* **6**, 773–775.

Higuera, M., Nicolás, J. & Vega, J. 1994 Linear oscillations of weakly dissipative axisymmetric liquid bridges. *Phys. Fluids* **6**, 438–450.

Jackson, H. W., Barmatz, M. & Shipley, C. 1988 Equilibrium shape and location of a liquid drop acoustically positioned in a resonant rectangular chamber. *J. Acoust. Soc. Am.* **84**, 1845–1862.

Lowry, B. J. & Steen, P. H. 1995 Flow-influenced stabilization of liquid columns. *J. Colloid Interface Sci.* **170**, 38–43.

Lowry, B. J. & Steen, P. H. 1997 Stability of slender liquid bridges subjected to axial flows. *J. Fluid Mech.* **330**, 189–213.

Marston, P. L. 1980 Shape oscillation and static deformation of drops and bubbles driven by modulated radiation stresses - Theory. *J. Acoust. Soc. Am.* **67**, 15–26.

Marston, P. L. & Apfel, R. E. 1979 Acoustically forced shape oscillation of hydrocarbon drops levitated in water. *J. Colloid Interface Sci.* **68**, 280–286.

Marston, P. L., Trinh, E. H., Depew, J. & Asaki, T. J. 1994 Response of bubbles to ultrasonic radiation pressure: dynamics in low gravity and shape oscillations. In *Bubble Dynamics and Interface Phenomena: Proc. IUTAM Symp.* (ed. J. R. Blake, J. M. Boulton-Stone & N. H. Thomas), pp. 343–353. Kluwer.

Morse, S. F., Thiessen, D. B. & Marston, P. L. 1996 Capillary bridge modes driven with modulated ultrasonic radiation pressure. *Phys. Fluids* **8**, 3–5.

Nicolás, J. A. 1992 Magnetohydrodynamic stability of cylindrical liquid bridges under a uniform axial magnetic field. *Phys. Fluids* A **4**, 2573–2577.

Oldham, K. B. & Spanier, J. 1974 *The Fractional Calculus.* Academic.

Papoulis, A. 1962 *The Fourier Integral and its Applications.* McGraw-Hill.

Perales, J. M. & Meseguer, J. 1992 Theoretical and experimental study of the vibration of axisymmetric viscous liquid bridges. *Phys. Fluids* A **4**, 1110–1130.

Plateau, J. A. F. 1863 Experimental and theoretical researches on the figures of equilibrium of a liquid mass withdrawn from the action of gravity. *Ann. Rep. Board of Regents of the Smithsonian Institution*, pp. 207–285. Washington, DC.

Prosperetti, A. 1977 Viscous effects on perturbed spherical flows. *Q. Appl. Maths* **34**, 339–352.

Raco, R. J. 1968 Electrically supported column of liquid. *Science* **160**, 311–312.

Ramos, A., Gonzalez, H. & Castellanos, A. 1994 Experiments on dielectric liquid bridges subjected to axial electric fields. *Phys. Fluids* **6**, 3206–3208.

Rayleigh, Lord 1879 On the instability of jets. *Proc. Lond. Math. Soc.* **10**, 4–13.

Sankaran, S. & Saville, D. A. 1993 Experiments on the stability of a liquid bridge in an axial electric field. *Phys. Fluids* A **5**, 1081–1083.

Sanz, A. 1985 The influence of the outer bath in the dynamics of axisymmetric liquid bridges. *J. Fluid Mech.* **156**, 101–140.

Sanz, A. & Díez, J. L. 1989 Non-axisymmetric oscillations of liquid bridges. *J. Fluid Mech.* **205**, 503–521.

Shi, X., Brenner, M. & Nagel, S. 1994 A cascade of structure in a drop falling from a faucet. *Science* **265**, 219–222.

Stroud, J. S. & Marston, P. L. 1993 Optical detection of transient bubble oscillations associated with the underwater noise of rain. *J. Acoust. Soc. Am.* **94**, 2788–2792.

Tjahjadi, M., Stone, H. & Ottino, J. 1992 Satellite and subsatellite formation in capillary breakup. *J. Fluid Mech.* **243**, 297–317.

Trinh, E. H., Marston, P. L., Robey, J. L. 1988 Acoustic measurement of the surface tension of levitated drops. *J. Colloid Interface Sci.* **124**, 95–103.

Trinh, E. H., Zwern, A. & Wang, T. G. 1982 An experimental study of small-amplitude drop oscillations in immiscible liquid systems. *J. Fluid Mech.* **115**, 453–474.

Wang, T. G., Anilkumar, A. V. & Lee, C. P. 1996 Oscillations of liquid drops: results from USML-1 experiments in space. *J. Fluid Mech.* **308**, 1–14.

Yosioka, K. & Kawasima, Y. 1955 Acoustic radiation pressure on a compressible sphere. *Acustica* **5**, 167–173.

Zhang, X., Padgett, R. S., & Basaran, O. A. 1996 Nonlinear deformation and breakup of stretching liquid bridges. *J. Fluid Mech.* **329**, 207–245.

Zhang, Y. & Alexander, J. I. D. 1990 Sensitivity of liquid bridges subject to residual axial acceleration. *Phys. Fluids* A **2**, 1966–1974.